Hindawi

Research Article

Theoretical Modeling of Composite Micro- and Nano-Fiber Devices and Electronic Information Application Research

Haibin Yang and Zhidong Liu [ID]

Electrical and Information Engineering College, Jilin Agricultural Science and Technology University, Jilin, 132101 Jilin, China

Correspondence should be addressed to Zhidong Liu; liuzhidong@jlnku.edu.cn

With the continuous development of information science and technology, micro- and nano-fiber optic sensing technology has been widely used in the fields of medicine, communication engineering, and environmental monitoring, and fiber optic devices are widely available in the market because of their advantages such as anti-magnetic interference, corrosion resistance, light weight, high sensitivity, and transmission bandwidth. The purpose of this paper is to investigate the intrinsic correlation between micro- and nano-optical fiber devices and electronic information, introduce the fabrication process of micro- and nano-optical fiber, numerical simulations, and corresponding magnetic field experiments, explore the effects of polarization dispersion and polarization-related dissipation on the system, and enhance the sensing characteristics of micro- and nano-optical fiber through experimental design to maximize its functionality. The experimental results show that the refractive index and magnetic field exhibit a linear relationship with correlation coefficients of 0.995 and 0.994, respectively, when the external magnetic field is between 70 Oe and 300 Oe.

1. Introduction

1.1. Background. Fiber optic technology began in the 1950s, the essence of the medium optical waveguide, while optical fiber is the study of the transmission and exchange of light, the emergence of low-loss optical fiber in the 1970s to promote the development of fiber optic technology [1, 2]. With the continuous progress of science and technology, the convenience of the use of tools has become the mainstream trend, but also continue to become the direction of the scientific community continue to research, the use of tools more and more integrated to meet the needs of the times, micro-fiber optic technology has become the subjects of research, in this context, micro- and nano-fiber optic technology into the field of vision, due to the continuous in-depth research found that micro- and nano-fiber optic technology can form different functions of micro- and nano-photonics devices. It has different degrees of impact on many modern industries, and from this perspective, there is a real need for the development of micro- and nano-fiber optic technology.

1.2. Significance. With the continuous development of micro- and nano-fiber technology, researchers have found that micro- and nano-fibers have many interesting properties [3, 4]. When the diameter of the fiber reaches the micro-nano-scale, the outer diameter of the optical fiber is generally 125-140 μm, and the core diameter is generally 3-100 μm and when the diameter is kept within a certain range, the binding of the optical field is stronger than that of an ordinary fiber, which can enhance the interaction between light and the medium and produce nonlinear effects at lower input power; it can transfer the energy force of the optical field to propagate outside the fiber, and this energy can be used as a sensitive sensor material for light coupling in certain cases.

1.3. Related Work. Micro- and nano-fiber optic technology is relevant in real life, but because of its late appearance, many functions are still being explored and have led to numerous studies. XIA presents different micro- and nano-structured fiber optic probes for biosensing, imaging, and stimulation applications and argues that modifications to the fiber can

extend the design freedom from waveguide optimization to functional material integration, and that fiber optic probes with optimized waveguide structure or integrated functional materials of fiber optic probes can achieve enhanced optical mode interaction with biological samples, leading to ultra-sensitive biosensors with significantly low detection limits [5]. Jiang J proposed an optical detection method based on micro- and nano-fiber (MNF) technology through a simple single-mode fiber. Theoretically, the evaporation field generated by MNF is calculated and its relationship with refractive index and water in oil is established, after which a MNF probe with a diameter of $800 - 125\mu$m is fabricated and prepared by means of a home-made melt-tapered platform. The experimental results showed that the MNF-based optical sensor could achieve real-time measurement of moisture in transformer oil with a sensitivity of 1.8 ppm when the MNF diameter was 800 nm [6]. May-Arrioja D. A. presented experimental results of an optical fiber pressure sensor based on multimode interference effects (MMIs). The key component is a small multimode fiber (MMF) part without cladding, which is placed in direct contact with a polydimethylsiloxane polymer layer previously attached to a pressure-sensitive membrane. As the applied pressure increases, both the polymer contact area and the induced stress on the MMF increase in proportion to the applied pressure. The response of the sensor is highly linear over the pressure range of 0-960 kPa with a sensitivity of -0.145×10-3 mW/kPa. The main features of the MMI pressure sensor are its low cost and high repeatability [7]. Liu presented recent research advances in key devices and technologies for fiber optic sensor networks (FOSN). As the most important devices for FOSN, a variety of light sources have been developed, including broadband multi-wavelength fiber lasers operating in C-band, switchable tunable 2-μm multi-wavelength fiber lasers, ultrafast mode-locked fiber lasers, and optical broadband chaotic sources with very promising applications in FOSN [8]. Krehlik P. provided an overview of an electronically stabilized (ELSTAB) fiber time and frequency (T& F) distribution system, which is based on the idea of using variable electronic delay lines as compensation elements, describes various extensions of the basic system that allow the creation of a long-range multi-user network, discusses the fundamental limitations of the approach caused by fiber dispersion and system dynamics, and outlines the main hardware challenge of the system, which is the design of a pair of low-noise, precisely matched delay lines. Finally, experimental results of T&F distribution over a 615 km long fiber are presented, demonstrating an average frequency stability of 105 s and a time calibration well below 50 ps accuracy in the range of 1-7×10-17 [9]. Pimentel R presents a cost-effective bridge crane (B-WIM) system for identifying train loads using fiber optic technology. The system is capable of estimating the speed, geometry, and static axle loads of trains using an algorithm proposed by Moses. The algorithm involves solving a reverse identification problem where the measured structural response is known and the load scenario is unknown. The method relies on the concept of the influence line (IL), which is estimated from the passage of a calibrated vehicle with known characteristics

[10]. An innovative reversible data hiding (RDH) scheme is proposed which uses Lagrangian interpolation polynomials, secret sharing, and bit permutation to achieve electronic medical security. The covered medical images are subsampled into four shares, and cloud computing with Internet proves to be an important tool for providing better healthcare services. However, the maintenance, privacy, confidentiality, and security of electronic health information (EHI) pose a huge challenge for telemedicine. The scheme is used to expand subsamples to hide EHI, and secret information is processed using Lagrangian interpolation polynomials before being embedded in various cover images [11]. Wang presented the principle of holographic lithography and described its application in fabricating various micro- and nano-photonic structures such as 3D face-centered cubes, wooden piles, diamond-like photonic crystals, and quasi-crystalline structures, chiral metamaterials, and periodic defect mode structures, and holographic lithography is a low-cost, time-saving, and efficient microfabrication method with promising applications in making metamaterials and photonic crystal templates [12]. Micro- and nano-photonic structures are booming with a series of results in structural characterization, theory, and fabrication, but most of the high-quality photonic structures are artificial, and there are still some challenges in fabricating artificial large-area high-quality photonic materials.

1.4. Innovation Points. In this paper, we analyze the refractive index sensing characteristics of different types of single-mode fiber modes, think about the relationship between them in different cases, and verify the sensitivity of the refractive index through the experiment of interferometric instrumentation of different fibers; we propose a diameter-based fiber regulator to destroy the fiber by external force to change its original mode field distribution, and analyze its sensitivity in different cases through experiment. From this, the reasons for the change in transmission are explored.

2. Theoretical Modeling of Composite Micro- and Nano-Fiber Devices and Research Methods for Electronic Information Applications

2.1. Overview of Micro- and Nano-Optical Fibers. In the late 1870s, micro- and nano-fiber optic technology began to develop and was widely used in several fields, especially in the field of information applications [13]. Micro-nano-photonics mainly studies the law of interaction between light and matter at the micro-nano-scale and its applications in light generation, transmission, regulation, detection, and sensing. Micro-nano-photonics subwavelength devices can effectively improve the photonic integration, and it is expected to integrate photonic devices into a small single optical chip like electronic chips. Fiber optic technology is essentially a sensing technology, and the first controlled recordings appeared in the early 1990s, when some researchers proposed the use of glass fibers for medical
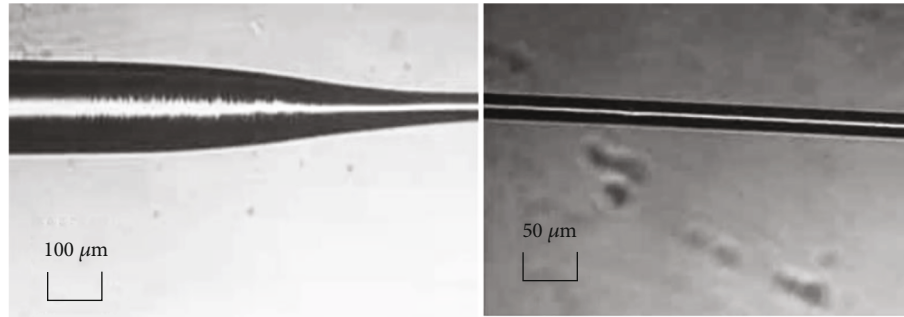
FIGURE 1: Micro-nano-area under optical microscope.

examinations, which led to the further development of micro- and nano-fiber optic technology in medicine. The difficulty of using light propagation is how to reduce transmission down loss and achieve optical communication. It was not until the continued maturation of fiber optic materials and wire drawing technology in 1972 that the low consumption of optical fibers was substantially advanced and successfully used to create a successful fiber optic communication system line, which laid the foundation for the practicalization of fiber optic communication [14].

Because fiber optic technology has many advantages such as high temperature and corrosion resistance and is widely used in real life, the survey data show that the global consumption of micro- and nano-fiber optic sensor market will grow at a rate of 20%, and the output value of about 5 billion U.S. dollars, in the Asia-Pacific region, China is the largest consumer and production market [15]. Photonic devices with many structures have been successfully made using micro- and nano-fiber technology, which have shown important research value in different fields such as communication and sensing, and more micro- and nano-fibers are designed and widely used. Microstructured fibers have been widely used in cutting-edge research in many fields such as optical communication, fiber sensing, and optical metrology, such as the generation of supercontinuum, high-power pulse transmission, ultra-low-power nonlinear effects, and tomography and remarkable results have been achieved in this research direction. Figure 1 shows the micro- and nano-regions under optical microscope.

2.2. Micro- and Nano-Fiber Mode Field Distribution. Micro- and nano-fibers are those whose diameters are infinitely converging to the micron or nanometer scale and whose refractive indices are relatively large. To explore the mode field distribution of micro- and nano-fibers, we first need to understand Maxwell's set of equations [16]. Figure 2 shows a schematic diagram of a micro- and nano-fiber.

First, we need to construct an ideal model of a micro- and nano-fiber, assuming that it can satisfy the following conditions.

(1) A diameter greater than 10 nm, which can respond to the optical field

(2) The micro-nano-fiber is relatively long, enough to establish a suitable mode field distribution

(3) The micro-nano-fiber indicates that it cannot be too coarse, but acceptable only to the extent that scattering of light is negligible

(4) The diameter of the micro-nano-fiber is uniformly distributed

Based on the above ideal state of the micro-nano-fiber, we can set the micro-nano-fiber as a cylinder, at which time the refractive index of the micro-nano-fiber can be segmented to represent.

$$t(a) = t_1, 0 < a < q, \tag{1}$$

$$t(a) = t_2, q < a < \infty. \tag{2}$$

In the above equation, q, t_1, and t_2 are the radius, core refractive index, and external ambient refractive index of the micro-nano-fiber, respectively. Fiber index of refraction generally refers to graded-index fiber. Graded-index fiber is also called self-focusing fiber. The center of refractive index of the fiber is the highest and decreases along the radial direction. The light beam propagates in the fiber and can be automatically focused without dispersion.

In general, neglecting their depletion, we express Maxwell's equations in the micro- and nano-fibers as follows: Maxwell's equations are a set of partial differential equations established by British physicist James Clark Maxwell in the 19th century to describe the relationship between electric and magnetic fields, charge density, and current density.

$$\left(\nabla^2 a^2 t^2 - \rho^2\right) \vec{b} = 0, \tag{3}$$

$$\left(\nabla^2 a^2 t^2 - \rho^2\right) \vec{k} = 0. \tag{4}$$

In the above expression, a is the refractive index of the point, $t = 2\pi\tau$, where τ is the wavelength and ρ is the wavelength propagation constant.
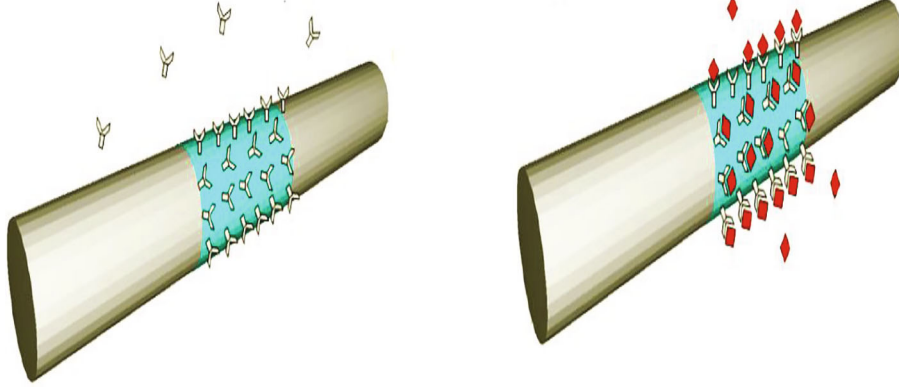
FIGURE 2: Schematic diagram of micro- and nano-fiber.

The eigenequation of the vector mode sum is expressed as:

$$\left[\frac{J'_Q(U)}{+}k'_Q(W) \right]\left[\frac{J'_Q(U)}{+}m^2{}_2 k'_Q(W) \right]$$
$$\left[UJ'_Q(U)WK_Q(K) \right]\left[UJ'_Q(U)m^2{}_1 WK_Q(K) \right]$$
$$= \left(\frac{v\alpha}{km_1} \right)^2 \left(\frac{V}{UK} \right)^4. \tag{5}$$

For PE_{0M} mode, there exists:

$$\frac{m_1{}^2 J_1(U){}_+ m_2{}^2 T_1(W)}{UJ_0(U)WK_0(W)} = 0. \tag{6}$$

For PN_{0M} mode, there exists:

$$\frac{J_1(U){}_+ T_1(W)}{UJ_0(U)WK_0(W)} = 0. \tag{7}$$

In the above equation, it denotes the Cybel function, $V = P_0 t(m_1^2 - m_2^2)/2$, $U = t(k_0^2 m_1^2 - \alpha^2)/2$, $W = t(\alpha^2 - k_0^2 m_2^2)/2$ where $t = 2b$.

Theoretically, optical fibers have many propagation modes, but only the transmission conditions and republican transmission modes can be propagated using optical fibers at the same time, and from this perspective, the propagation modes are not infinite. According to the number of transmission modes in the fiber, the fiber can be divided into multimode fiber and single-mode fiber. At a certain operating wavelength, multimode fiber is a dielectric waveguide that can transmit many modes, while single-mode fiber only transmits the fundamental mode. In micro- and nano-optics, the accommodation mode depends on the radius and refractive index of the micro- and nano-optics [17]. The expression for the refractive index of micro- and nano-optics medium is as follows:

$$\Delta m = m_1 - m_2. \tag{8}$$

The expression of the fundamental mode energy condition of the micro- and nano-fiber is:

$$W = \pi \frac{f_{AZ}}{\mu_0}\left(m_1^2 - m_2^2 \right) \approx 2.40, \tag{9}$$

where $f_{AZ} = 2b$ denotes the critical diameter of the micro- and nano-fiber.

The expressions for each component of the electric field transmitted in a micro- and nano-fiber can be expressed as:

$$e_t = -\frac{c_1 J_0(UR) + c_2 J_2(UR)}{J_1(U)} f_1(u), \tag{10}$$

$$e_u = -\frac{c_1 J_0(UR) - c_2 J_2(UR)}{J_1(U)} g_1(u), \tag{11}$$

$$e_p = -i\frac{U J_1(UR)}{\mu\sigma J_1(U)} f_1(u), \tag{12}$$

where $0 \leq c < q$;

$$e_t = -\frac{Uc_1 K_0(WR) - c_2 k_2(WR)}{WK_1(W)} f_1(u), \tag{13}$$

$$e_u = -\frac{Uc_1 k_0(WR) + c_2 k_2(WR)}{Wk_1(W)} g_1(u), \tag{14}$$

$$e_p = -i\frac{Uk_1(WR)}{\tau\sigma k_1(W)} f_1(u). \tag{15}$$

For a micro-nano-fiber with uniform diameter and no significant folding, the expression can be expressed as:

$$T_{c1} = \frac{1}{2}\left(\frac{\gamma_0}{\pi_0} \right)^{0.5} \frac{lm_1^2}{\alpha J_1^2(R)} * \left[c_1 c_3 J_0^2(RF) + c_2 c_4 J_2^2(RF) \right.$$
$$\left. + \frac{1 - A_1 A_2}{2} J_0(RF)J_2(RF)\cos(2\theta) \right]. \tag{16}$$
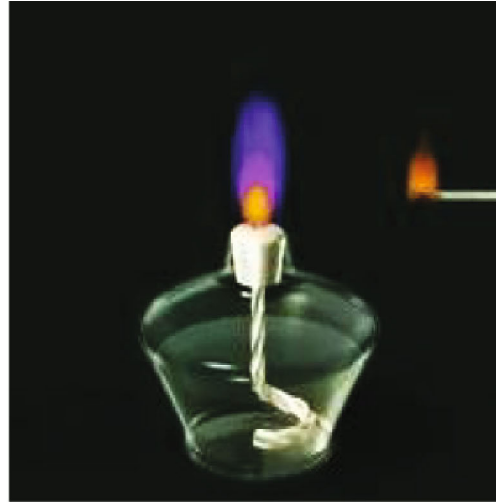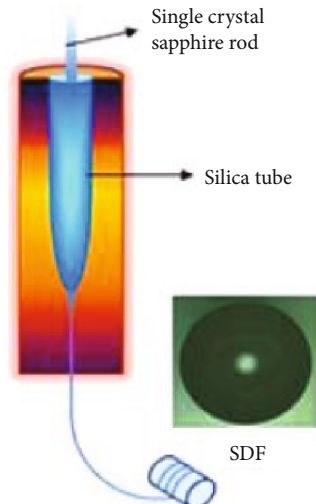
Figure 3: Machining tools and materials.

At this point, $0 \leq c < q$.

$$
T_{c2} = \frac{1}{2} \left(\frac{\gamma_0}{\pi_0} \right)^{0.5} \frac{lm_1^2 U^2}{\alpha L_1^2(W) W^2} * \left[c_1 c_5 l_0^2(WF) + c_2 c_6 l_2^2(WF) \right.
$$
$$
\left. + \frac{1 - 2\Delta - A_1 A_2^2}{2} L_0(WF) L_2(WF) \cos 2\theta \right].
$$
(17)

At this point, $q \leq c < \infty$.

2.3. Electronic Information. "Electronic information" is an informatics vocabulary, and its appearance is closely related to the rapid development of computer technology, communication technology, and high-density storage technology and its wide application in various fields. Electronic information engineering is a discipline that applies computer and other modern technologies for electronic information control and information processing. It mainly studies the acquisition and processing of information, and the design, development, application, and integration of electronic equipment and information systems.

2.4. Preparation Methods of Micro- and Nano-Optical Fibers. Micro- and nano-optical fibers are circular optical waveguides with diameters in the micron range. Since the introduction of micro- and nano-fiber technology, researchers have explored a variety of methods for fabricating micro- and nano-fibers. In terms of specific practice, there are only two methods to fabricate micro-nano-constructions: top-to-bottom and bottom-to-bottom. The process of making optical fiber by chemical growth method is a bottom-to-top process, and the micro-nano-fiber drawn from bulk glass is a top-to-bottom process. It is customary for us to refer to the process of fabricating micro- and nano-fibers using chemical techniques as bottom-up. Other technologies manufacture processes called top-to-bottom processes whose

main raw materials include, but are not limited to, block glass and single-mode fibers [18, 19].

2.4.1. Single-Mode Fiber Fabrication. The fabrication of micro- and nano-optical fibers using flame heating hair was first proposed in 2003. This method mainly uses an alcohol lamp for heating; first, a small section of fiber is heated until it melts, and then tension is applied to both ends of the fiber until the desired diameter of the micro-nano-fiber is obtained. If we want to make it very light, the heating and melting operation in the natural environment is very easy to be affected by the external environment; secondly, when applying tension to the micro-nano-fiber, we need to keep the tension constant, then there is a great limitation of this method when we need to make a finer diameter, and the micro-nano-fiber is easy to break if we are not careful, so this method is only applicable to the ideal state, and it is very difficult to do in practice [20, 21]. When heating the single-mode fiber, a certain stretching force is applied to both ends of the single-mode fiber, and the pulling force can be kept constant by controlling the stretching speed. Figure 3 shows the processing tools and materials:

2.4.2. Block Glass Fabrication. In addition to single-mode fiber fabrication, researchers have proposed that bulk glass can be used as a material for micro-nano-fiber preparation, and this method has a wide selection of materials, including sulfide glass, fluoride glass, and tellurite glass, among others, and the desired substances, such as ions, can be added to these materials, so that the fabricated micro-nano-fiber can be more complete during the fabrication process [22]. The steps are as follows.

(1) First, the micro-nano-fiber is heated, noting that the melting point at this point must be greater than that of the chosen glass material

(2) Contacting the bulk glass with the heated fiber while continuing to maintain the high temperature of the micro-nano-fiber
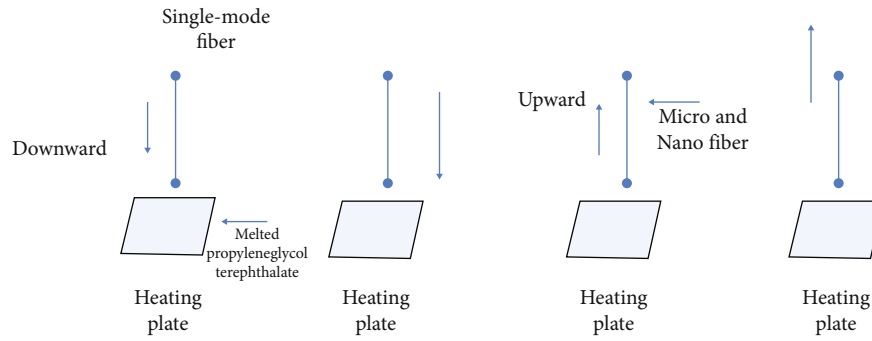
FIGURE 4: . Operation schematic.

(3) Take away the lump glass when the mutual contact appears to be melted, but it must be confirmed that there is a small portion of melted glass material on the micro-nano-fiber at this time

(4) Pacing the new micro-nano-fiber in contact with the heated micro-nano-fiber

(5) Lowering the heating temperature to cool down the glass between the two micro-nano-fibers

(6) The application of a certain rate of pulling from unheated micro-nano-fibers results in new micro-nano-fibers. Using this method of fabrication, micro-nano-fibers with different characteristics can be produced depending on the materials chosen

2.4.3. Polymer Fabrication. In addition to the above-mentioned raw materials, researchers have found that polymers can also be used to fabricate micro- and nano-fibers. In the early days, micro- and nano-optical fibers have been successfully fabricated using polypropylene terephthalate polymers. The low melting point, good flexibility, and fast crystallization rate of poly (propylene terephthalate) make it possess the requirements for fiber formation, and the refractive index of poly (propylene terephthalate) is only 1.638 when it is in the amorphous state, which possesses good optical confinement [23, 24]. The manufacturing steps are as follows.

(1) Firstly, poly (propylene terephthalate) is heated to a softened state in which the temperature is kept stable

(2) Contacting the melted poly (propylene terephthalate) with a single-mode optical fiber, at which point the single-mode fiber will have some residue of the poly material

(3) Lifting the single-mode fiber at this time at a certain speed

After lifting the single-mode fiber, an intuitively very fine micro-nano-fiber will appear, and it will rapidly cool down into an amorphous poly (propylene terephthalate) micro-nano-fiber. Figure 4 shows a schematic diagram of the operation:

2.4.4. Laser Preparation. Since the use of gas for heating is susceptible to interference from the external environment and can easily cause errors during preparation, researchers have worked to find fabrication methods that are free from interference from the external environment, and in 2006 successfully fabricated micro-nano-fibers using a carbon dioxide laser as a heating instrument, which uses a carbon dioxide laser to scan and heat a single-mode fiber [25]. The main principle is to adjust the output of the carbon dioxide laser with a total controller, and use a tool to focus the laser on a single-mode fiber, and the spot diameter matches the micro-nano fiber used. By controlling the angle of the tool, the entire light spot in the single-mode fiber can move axially, and the heating of the single-mode fiber needs to change the structure; the longer the micro-nano-fiber needed, then the higher the power output of the CO2 laser needs to be, but this method is not infinitely long, and the diameter of the pulled micro-nano-fiber is still said to be relatively large compared to other methods [27].

2.4.5. Electrode Heating Preparation. To understand the problem of interference from the external environment, in addition to using a CO2 laser, researchers have proposed to protest the use of electrodes for heating; the main steps of which are as follows.

(1) First fixing the single-mode fiber with one end placed in a heater

(2) Using a heater bar to press the single-mode fiber into the container, the heater bar needs to be connected to the electrode with a standard voltage of 250 V. The temperature of the heated container needs to reach 1600°C

(3) The other end of the micro-nano-fiber is fixed on the rotating platform, and the rotating platform is driven to rotate after reaching a certain temperature, and the heated single-mode fiber can be drawn out of the micro-nano-fiber during the rotation process

The micro-nano-fiber prepared using this heating method can reach 900 nm in diameter and several hundred mm in length, and the heating of the single-mode fiber using electrodes can provide a large heating area and make the

TABLE 1: Comparison of various micro- and nano-fiber drawing methods.

| Preparation method	Two-part pulling method	Self-adjusting pulling method	Block glass drawing	Polymer drawing	Laser pulling	Electrode heating and drawing
Micro- and nano-fiber diameter (nm)	49	19	49	65	3000-39985	893
Transmission loss	0.008 dB/nm	*	0.01 dB/nm	0.01 dB/nm	0.06 dB/nm	0.01 dB/nm
Features	Easy and convenient	Minimal diameter	Multi-doped micro- and nano-fibers	Low melting point	Overcoming environmental interference	Longest length
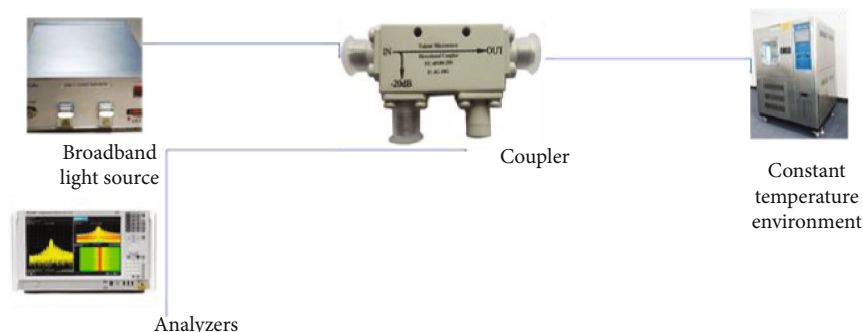
FIGURE 5: Schematic diagram of the test system.

TABLE 2: Relative humidity values of salt solutions.

Solution		Magnesium chloride	Lithium chloride	Potassium carbonate	Sodium chloride
	26°C	32.3	11.1	43.5	75.1
Relative humidity (%)	29°C	32.1	11.2	43.5	75.2
	30°C	32	11.2	43.5	75.2

single-mode fiber uniformly heated; in this process, the user can change the voltage as well as the rotating platform to change the length and diameter of the micro-nano-fiber [28]. Table 1 shows the comparison of various micro- and nano-fiber drawing methods:

3. Experiments on Theoretical Modeling of Composite Micro- and Nano-Fiber Devices and Electronic Information Applications

3.1. Experimental Environment. The micro-nano-fiber sensor is put into different humidity devices, and the data acquisition connector is connected to the broadband light source and the spectrum analyzer through a 3 dB coupler, and the humidity environment in the experiment uses a supersaturated solution, and we select different supersaturated solutions such as sodium chloride, potassium carbonate, magnesium chloride, and lithium chloride for the experiment, keeping the experimental temperature between 26°C and 29°C [29]. If the temperature of the chemical solution is too low or too high, a chemical reaction will occur, resulting in the deterioration of the solution, and deviations will occur in the experiment. The experimental setup is shown in Figure 5.

3.2. Experimental Data Acquisition. Table 2 shows supersaturated solutions with different humidity levels, and in our experiments, we passed sensors with different specifications through these supersaturated solutions in sequence, labeled separately, at different temperatures, and the wavelength of the micro-nano-fiber changed as the humidity of the solution varied [30]. The wavelength of magnesium chloride solution will shorten as the temperature increases, and other solutions will remain unchanged or elongated.

According to the data in Table 3, it can be seen that the wavelengths of the micro-nano-fibers were significantly shifted by adding them to different supersaturated solutions while keeping the experimental temperature constant, but they basically drifted toward the long wave direction. In addition, with the increase of ambient humidity, the center wavelength of the reflection spectrum of the humidity sensor shifts to the long wavelength direction.

According to the data in Table 4, it can be seen that different micro-nano-optical fibers change in different supersaturated solutions while keeping the experimental temperature constant, and overall, when the temperature is constant, the greater the relative humidity of the solution, then the greater the amount of drift to come, and according to the experiment, it can be seen that the larger drift occurs

TABLE 3: Wavelengths of saturated solutions with different humidity.

Solution	Magnesium chloride	Lithium chloride	Potassium carbonate	Sodium chloride
Temperature ($^{\circ}$C)	25	25	25	25
Wave length (nm)	1530	1537	1538	1536
Loss (db)	50	35	45	40

TABLE 4: Wavelength drift.

Solution	Magnesium chloride	Lithium chloride	Potassium carbonate	Sodium chloride
Temperature ($^{\circ}$C)	25	25	25	25
Wet relative humidity (%)	10	30	50	70
Wavelength drift amount (nm)	0	0.2	0.7	1.3

TABLE 5: Sensor corresponding parameters.

Sensors	Micro- and nano-fiber diameter (μm)	Sensitivity (pm/%)	Linearity (%)
Magnesium chloride	115	23.12	99.61
Lithium chloride	23	31.75	99.59
Potassium carbonate	17	32.18	99.29
Sodium chloride	14	35.46	99.73

in magnesium chloride, followed by sodium chloride solution, and the smallest drift occurs in lithium chloride solution [31].

According to the data in Table 5, it can be seen that the sensitivity of the sensors used in the experiments is above 99%, and most of the humidity sensors are higher than the sensitivity of ordinary optical fiber humidity sensors, so it can be concluded that the sensor sensitivity of micro-nano-fiber humidity sensitivity has been improved to a great extent compared with ordinary micro-nano-fiber. Combined with the above mentioned that within a certain humidity, the wavelength drift amount and humidity have a good linear relationship, so we believe that the humidity sensor has good detection effect in a certain acidic solution environment [32].

4. Theoretical Modeling and Electronic Information Application Research Analysis of Composite Micro- and Nano-Fiber Devices

4.1. Micro- and Nano-Optical Fiber Stability Characteristics. In the above experiments, we introduced that wavelength and refractive index are length dependent. If the length is simply changed, then the wavelength also changes, and in order to explore the relationship, we utilized an interferometer axial strain characteristic measurement instrument for detection (Figure 6 shows the interferometer axial strain system) each time the position is shifted and its length is changed, and the following data are obtained.

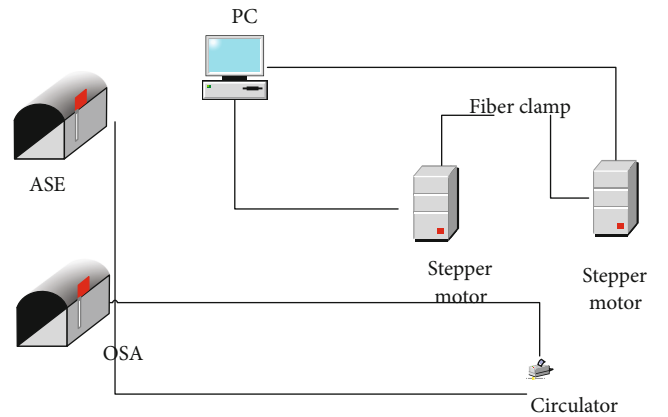According to Figure 7, we can see that we have carried out the projection profiles during the changes of 80 μm,

FIGURE 6: Interferometer axial strain system.

160 μm, 240 μm, and 320 μm, respectively, and from the data, we can see that the difference in the values of the spectral interference valley drift is relatively small in different length displacement changes, and overall it is still relatively stable and basically does not change much according to the valley comparison, so that it can be used as a strainer [33].

According to the data variation in Figure 8, we can find that analyzing the ratio of the length of the axial change to the length of the fiber can be derived from the microstrain of the fiber axially, and according to the recorded changes corresponding to the wavelengths shown in the figure, we can see that the reasonable sensitivity of the interferometer is around 0.55, while the sensitivity of the interferometer we obtained is around 0.6 and 0.61, so we can confirm that the sensitivity is reasonable at this time.
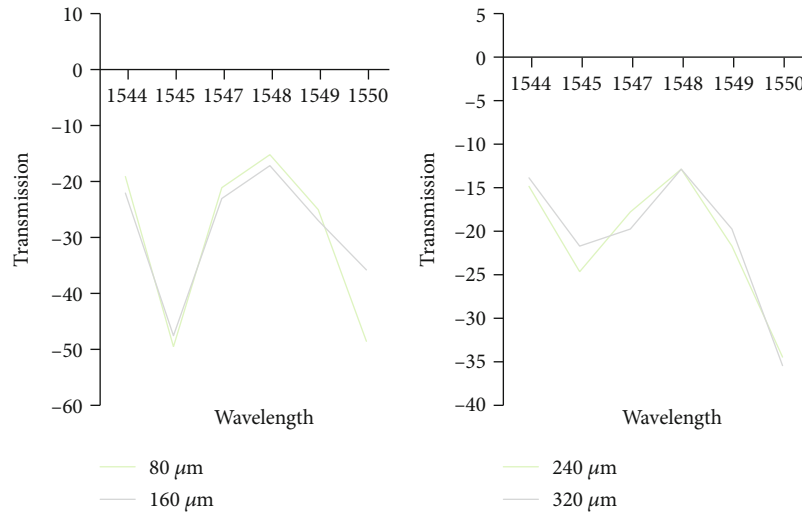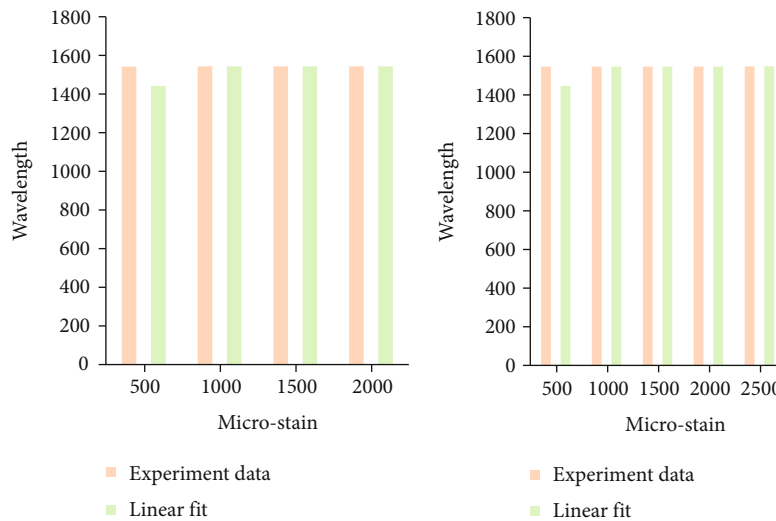
Figure 7: Microstrain measurement.

Figure 8: Relationship between wavelength and strain variation.

4.2. The Magnetic Field of Micro- and Nano-Fibers. As mentioned in the previous section, the magnetic field of micro-nano-fiber is closely related to the fiber diameter and core refractive index. According to the analysis in the study, chemical means can be used to change the diameter of the micro-nano-fiber as a way to change the whole magnetic field distribution, and in order to verify this conjecture, we conducted an experimental analysis and found that the diameter size of the micro-nano-fiber does have a large influence on the whole magnetic field [34].

According to Figure 9, when the corrosive solution is contacted with the micro-nano-fiber, it is found that it has a large impact on the diameter of the micro-nano-fiber, resulting in a higher loss of the micro-nano-fiber, so it can be seen that the difference between the wave and valley in the figure is large, and once the external interference is performed, it will lead to a large change in its magnetic field; when the corroded micro-nano-fiber is added to the magnetic fluid solution when there is no external magnetic influ-

ence, its refractive index size remains at 1.4. When we add the magnetic fluid, it is obvious that the wavelength of the micro-nano-fiber has changed and the frequency has shifted.

4.3. Relationship between Magnetic Field Strength and Transmittance of Micro- and Nano-Fibers. In the above, we mentioned that the size of external magnetic field will cause the micro-nano-fiber to change to different degrees, and by adding different properties of magnetic fluid can make the refractive index of the micro-nano-fiber change, and when the refractive index changes, its transmittance will also change, and the main changes are as follows:

From Figure 10, it can be seen that the influence of the magnetic field size on the transmittance, but according to the obtained data, we find that the transmittance presents a nonlinear relationship; when the external magnetic field is less than a certain data, the transmittance will remain unchanged, and when the external magnetic field reaches the degree of saturation, its transmittance does not change
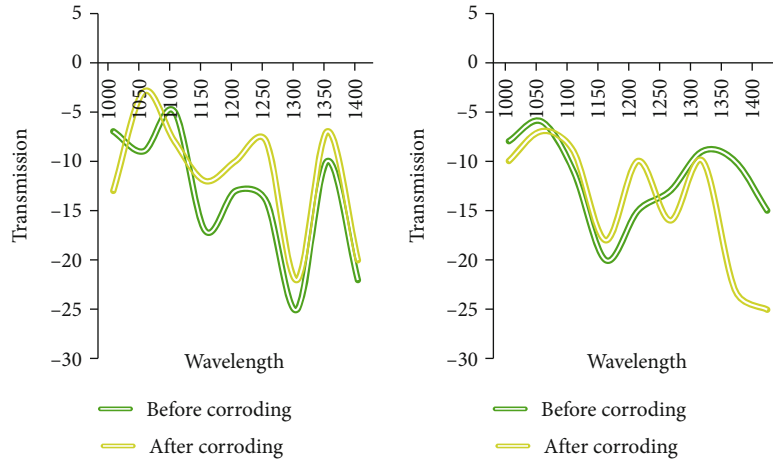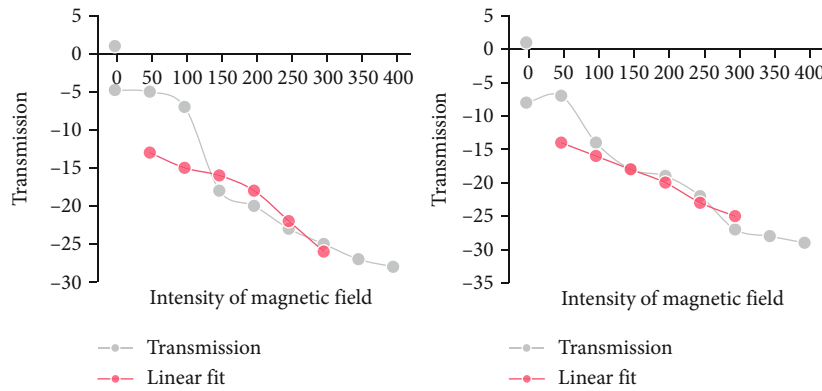
FIGURE 9: Comparison chart of corroded fiber.

FIGURE 10: Comparison of magnetic field strength and transmittance.

significantly, but when the external magnetic field is between 70 Oe and 300 Oe. However, when the external magnetic field is between 70 Oe and 300 Oe, they show a certain linear relationship with correlation coefficients of 0.995 and 0.994, respectively. This data indicates that the relationship of the optical magnetic field can be adjusted by using different degrees of external magnetic field and can be applied in the communication magnetic field.

5. Conclusions

With the continuous development of micro- and nano-fiber technology, fiber optic devices are gradually adding to the convenience of miniaturization, and in the process of continuous miniaturization, micro- and nano-fiber technology is also developing, and micro- and nano-fibers of different structures, diameters, and lengths are being manufactured continuously, and at present, the academic exploration of the characteristics of micro- and nano-fibers with differences in fabrication and the application of devices in different fields has become the current fiber optic science and technology and scientific. In this paper, we will focus on the fabrication of micro- and nano-fibers. In this thesis, we have (1) investigated the fabrication methods of micro-

and nano-fibers in different transmission modes, and analyzed their physical significance, advantages, and disadvantages in the practical process, and their practical value; (2) explored the transmission characteristics of fine core micro- and nano-fibers with different diameters and their distribution characteristics, and simulated the transmission modes of different sizes of micro- and nano-fibers; (3) investigated the connection between the magnetic field of micro- and nano-fibers and fiber diameter, core refractive index, and found the connection between the magnetic field of micro- and nano-fibers. The larger the diameter of the micro-nano-fiber, the larger the wavelength shift, and the corresponding change in refractive index, thus changing the magnetic field; (4) to explore the correlation between the magnetic field and transmittance, it is found that when the external magnetic field is less than a certain data, the transmittance will remain unchanged, and when the external magnetic field reaches saturation, the transmittance does not change significantly, but when the external magnetic field is between 70 Oe and 300 Oe, the transmittance does not change significantly. However, when the external magnetic field is between 70 Oe and 300 Oe, they show a certain linear relationship. Although this paper has explored certain contents, there are still many shortcomings: (1) the operation

steps of the micro-nano-fiber research in this paper are all in the ideal experimental environment, the encapsulation technology of micro-nano-fiber needs a constant temperature environment, and due to this necessary condition, it cannot be utilized in a commercial environment on a large scale; (2) when using chemical technology for corrosion, it is easy to make mistakes, and the corrosion solution. We still need to find other relatively safe methods to fabricate micro-nano-fibers; (3) the techniques adopted in this paper are considered to be operational, which makes it difficult to ensure that the fabricated micro-nano-fibers are identical, which makes it more difficult to mass produce micro-nano-fibers.

Data Availability

The data that support the findings of this study are available from the corresponding author upon reasonable request.

Conflicts of Interest

The authors declared no potential conflicts of interest with respect to the research, authorship, and/or publication of this article.

References

[1] H. Song and M. Brandt-Pearce, "Range of influence and impact of physical impairments in long-haul DWDM systems," *Journal of Lightwave Technology*, vol. 31, no. 6, pp. 846–854, 2013.

[2] H. Song and M. Brandt-Pearce, "A 2-D discrete-time model of physical impairments in wavelength-division multiplexing systems," *Journal of Lightwave Technology*, vol. 30, no. 5, pp. 713–726, 2012.

[3] B. Gao, X. Ning, and P. Xing, "Shock wave induced nanocrystallization during the high current pulsed electron beam process and its effect on mechanical properties," *Materials Letters*, vol. 237, no. 15, pp. 180–184, 2019.

[4] G. Bo, L. Chang, H. Chenglong et al., "Effect of Mg and RE on the surface properties of hot dipped Zn–23Al–0.3Si coatings," *Science of Advanced Materials*, vol. 11, no. 4, pp. 580–587, 2019.

[5] X. Yu, S. Zhang, M. Olivo, and N. Li, "Micro- and nano-fiber probes for optical sensing,imaging, and stimulation in biomedical applications," *Photonics Research*, vol. 8, no. 11, pp. 104–125, 2020.

[6] J. Jiang, X. Wu, Z. Wang, C. Zhang, G. Ma, and X. Li, "Moisture content measurement in transformer oil using micro-nano fiber," *IEEE Transactions on Dielectrics and Electrical Insulation*, vol. 27, no. 6, pp. 1829–1836, 2020.

[7] D. A. May-Arrioja, V. I. Ruiz-Perez, Y. Bustos-Terrones, and M. A. Basurto-Pensado, "Fiber optic pressure sensor using a conformal polymer on multimode interference device," *IEEE Sensors Journal*, vol. 16, no. 7, pp. 1956–1961, 2016.

[8] D. Liu, Q. Sun, P. Lu, L. Xia, and C. Sima, "Research progress in the key device and technology for fiber optic sensor network," *Sensors*, vol. 6, no. 1, pp. 1–25, 2016.

[9] P. Krehlik, Ł. Śliwczyński, Ł. Buczek, J. Kołodziej, and M. Lipiński, "ELSTAB—fiber-optic time and frequency distribution technology: a general characterization and fundamental limits," *IEEE transactions on ultrasonics, ferroelectrics, and frequency control*, vol. 63, no. 7, pp. 993–1004, 2016.

[10] R. Pimentel, D. Ribeiro, L. M. Matos, A. Mosleh, and R. Calçada, "Bridge Weigh-in-Motion system for the identification of train loads using fiber-optic technology," *Structure*, vol. 30, no. 1, pp. 1056–1070, 2021.

[11] R. F. Mansour and S. A. Parah, "Reversible data hiding for electronic patient information security for telemedicine applications," *Arabian Journal for Science and Engineering*, vol. 46, no. 9, pp. 9129–9144, 2021.

[12] X. Wang, H. Lü, Q. L. Zhao, S. Y. Zhang, and W. Y. Tam, "Application progress of holographic lithghraphy in fabrication of micro-nano photonic structures," *Guang pu xue yu Guang pu fen xi= Guang pu*, vol. 36, no. 11, pp. 3461–3469, 2016.

[13] S. V. Kulakov, A. N. Yakimov, A. Bugaev, M. Postema, and V. B. Voloshinov, "Special issue: wave electronics and applications thereof in information and telecommunication systems," *Applied Acoustics*, vol. 112, p. 216, 2016.

[14] B. Wolf and C. Scholze, "Medicine 4.0: examples of applications of electronics, information technology and microsystems in modern medicine," *Medecine Sciences*, vol. 34, no. 11, pp. 978–983, 2018.

[15] G.-D. Peng, *Handbook of Optical Fibers*, Springer, Berlin/Heidelberg, Germany, 2018.

[16] Y. Qi, J. Zhang, Q. Feng, X. Zhang, Y. Liu, and Y. Han, "A novel high sensitivity refractive index sensor based on multicore micro/nano fiber," *Sensors*, vol. 9, no. 3, pp. 197–204, 2019.

[17] D. L. Costa, R. S. Leite, G. A. Neves, L. N. . L. Santana, E. S. Medeiros, and R. R. Menezes, "Synthesis of TiO_2 and ZnO nano and submicrometric fibers by solution blow spinning," *Materials Letters*, vol. 183, pp. 109–113, 2016.

[18] J. Amirian, S. Y. Lee, and B. T. Lee, "Designing of combined nano and microfiber network by immobilization of oxidized cellulose nanofiber on polycaprolactone fibrous scaffold," *Journal of Biomedical Nanotechnology*, vol. 12, no. 10, pp. 1864–1875, 2016.

[19] P. Carrera, P. J. Espinoza-Montero, L. Fernández, H. Romero, and J. Alvarado, "Electrochemical determination of arsenic in natural waters using carbon fiber ultra-microelectrodes modified with gold nanoparticles," *Talanta*, vol. 166, pp. 198–206, 2017.

[20] Y. Liu, A. Nguyen, A. Allen, J. Zoldan, Y. Huang, and J. Y. Chen, "Regenerated cellulose micro-nano fiber matrices for transdermal drug release," *Materials Science and Engineering C*, vol. 74, pp. 485–492, 2017.

[21] J. Han, D. Wang, and P. Zhang, "Effect of nano and micro conductive materials on conductive properties of carbon fiber reinforced concrete," *Nanotechnology Reviews*, vol. 9, no. 1, pp. 445–454, 2020.

[22] A. Kumar, M. P. Gupta, J. Banerjee et al., "Micro-welding of stainless steel and copper foils using a nano -second pulsed fiber laser," *Lasers in Manufacturing & Materials Processing*, vol. 6, no. 2, pp. 158–172, 2019.

[23] F. Xu, "Miniature function-integrated devices based on optical microfibers," *Yingyong Kexue Xuebao/Journal of Applied Sciences*, vol. 35, no. 4, pp. 469–502, 2017.

[24] F. P. Calmon, A. Makhdoumi, M. Medard, M. Varia, M. Christiansen, and K. R. Duffy, "Principal inertia components and applications," *IEEE Transactions on Information Theory*, vol. 63, no. 8, pp. 5011–5038, 2017.

[25] R. Zheng, Y. D. Liu, and H. Jin, "Optimizing non-coalesced memory access for irregular applications with GPU computing," *Frontiers of Information Technology & Electronic Engineering*, vol. 21, no. 9, pp. 1285–1301, 2020.

[26] T. R. Hu, J. B. Luo, H. Kautz, and A. Sadilek, "Home location inference from sparse and noisy data:models and applications," *Frontiers of Information Technology & Electronic Engineering*, vol. 17, no. 5, pp. 389–402, 2016.

[27] C. ILihong, "2 5- and 3-D TSV technology applications and failure analysis challenges," *Electronic Device Failure Analysis: A Resource for Technical Information and Industry Developments*, vol. 18, no. 3, pp. 54-55, 2016.

[28] Y. M. Yu and K. Kang, "Analysis and design of transformer-based CMOS ultra-wideband millimeter-wave circuits for wireless applications: a review," *Frontiers of Information Technology & Electronic Engineering*, vol. 21, no. 1, pp. 97–115, 2020.

[29] D. G. Nedumaran, M. A. Kumar, and M. Alaguraja, "Effect of mobile applications on farming in Virudhunagar District -a study," *SSRN Electronic Journal*, vol. 68, no. 1, pp. 12718–12727, 2020.

[30] W. B. Han, X. G. Chen, S. F. Li et al., "A novel non-volatile memory storage system for I/O-intensive applications," *Frontiers of Information Technology & Electronic Engineering*, vol. 19, no. 10, pp. 1291–1302, 2018.

[31] S. Khazaei and M. Rezaei-Aliabadi, "A rigorous security analysis of a decentralized electronic voting protocol in the universal composability framework," *Journal of Information Security and Applications*, vol. 43, pp. 99–109, 2018.

[32] R. A. Baryshev, S. V. Verkhovets, and O. I. Babina, "The smart library project: Development of information and library services for educational and scientific activity," *The Electronic Library*, vol. 36, no. 3, pp. 535–549, 2018.

[33] Y. C. Xie, H. Huang, Y. Hu, and G. Q. Zhang, "Applications of advanced control methods in spacecrafts:progress, challenges, and future prospects," *Frontiers of Information Technology & Electronic Engineering*, vol. 17, no. 9, pp. 841–861, 2016.

[34] M. B. Hariz and F. Bouani, "Synthesis and implementation of a fixed low order controller on an electronic system," *International Journal of System Dynamics Applications*, vol. 5, no. 4, pp. 42–63, 2016.